Electrochemical, theoretical, and structural investigations on the tetra cobalt "butterfly" Co4(CO)8L2(RC2R) (L = CO, PPh3; R = H, Et, Ph) clusters

Domenico. Osella, Mauro. Ravera, Carlo. Nervi, Catherine E. Housecroft, Paul R. Raithby, Piero. Zanello, and Franco. Laschi

Organometallics, **1991**, 10 (9), 3253-3259• DOI: 10.1021/om00055a049 • Publication Date (Web): 01 May 2002

Electrochemical, Theoretical, and Structural Investigations on the "Butterfly" $Co_4(CO)_8L_2(RC_2R)$ (L = CO, PPh_3; R = H, Et, Ph) Clusters

Domenico Osella,* Mauro Ravera, and Carlo Nervi

Dipartimento di Chimica Inorganica, Chimica Fisica e Chimica dei Materiali, Università di Torino, Via P. Giuria 7, 10125 Torino, Italy

Catherine E. Housecroft and Paul R. Raithby

University Chemical Laboratory, Lensfield Road, Cambridge CB2 1EW, U.K.

Piero Zanello and Franco Laschi

Dipartimento di Chimica, Università di Siena, Pian dei Mantellini 44, Siena, Italy

Received January 2, 1991

The butterfly clusters $Co_4(CO)_{10}(RC_2R)$ (R = H, Et, Ph) undergo two consecutive 1e reduction processes, the former being fully chemically and electrochemically reversible and the latter followed by a moderately fast chemical complication. The disubstituted cluster $Co_4(CO)_8(PPh_3)_2(HC_2H)$ has been synthesized and its solution- and solid-state structure determined by multinuclear NMR spectroscopy and single-crystal X-ray diffraction: monoclinic, $P2_1/n$ (No. 14), a = 11.491 (5) Å, b = 24.178 (8) Å, c = 15.998 (5) Å, β = 105.84 (3)°, V = 4275.9 (9) Å^3, Z = 4, R_F = 0.061. The substitution of PPh_3 for CO has occurred regiospecifically on both wing-tip cobalt atoms. The electrochemistry is qualitatively similar to that of the parent cluster, the reduction potentials being shifted toward more negative values. The strong influence of the substitution of PPh_3 for CO and the weak influence of the alkyne substituents on the reduction potentials suggest that the LUMO is metal core in character. This hypothesis is corroborated by ESR results on the radical monoanion and by theoretical calculations within the Fenske-Hall scheme.

Introduction

A number of organometallic species have now been characterized in which the tetrametallic frame has a "butterfly" configuration.[1]

This molecular arrangement can be viewed as a model for the chemisorption of unsaturated hydrocarbons over a step or kink of a metal surface.[2] Moreover, interest in such compounds has been stimulated by the report of enhanced reactivity for exposed carbidic carbon atoms in butterfly M_4C clusters.[3] It is conceivable that the butterfly configuration plays a subtle role in facilitating reaction of ligands bound between the "wings" and this role may be sensitive to electronic effects.[4] The butterfly clusters $Co_4(CO)_{10}$(alkyne)[5] (Figure 1) can be classified as a 60e molecule according to the EAN formalism, provided that the alkyne donates its four π electrons to the valence orbital of the M_4 frame, two electrons fewer than the 62e count usually associated with an open tetrahedron (five M-M bonds). The actual bonding scheme can be better described by the polyhedral skeletal electron pair (PSEP) approach;[6] the Co_4 butterfly clusters can be viewed as closo octahedron (S = 7, n = 6).

Since several examples of butterfly compounds having different ligands are now available, correlations between the dihedral angle (Φ) of the wings (a measurement of the tendency toward the planar configuration) and the electronic nature of such ligands have been proposed.[1,4] To our knowledge, three electrochemical investigations, a direct method to vary the electronic count of the clusters, have been so far reported[7-9] on this class of compounds.

Results and Discussion

Most of the electrochemical experiments have been carried out in CH_2Cl_2 solution since the cobalt butterfly clusters $Co_4(CO)_{10}(RC_2R)$ (R = H, **1**; R = Et, **2**; R = Ph, **3**) are unstable in more polar solvents such as acetone or acetonitrile.[10] However, $Co_4(CO)_8(PPh_3)_2(HC_2H)$ (**4**) is sufficiently stable in such solvents, and the electrochemical parameters are basically unchanged by a change of solvent.

The anodic cyclic voltammetry (CV) responses of all the $Co_4(CO)_{10}(RC_2R)$ (**1-3**) clusters in CH_2Cl_2 and at a Pt electrode are similar to those previously reported for the binary carbonyls $Co_4(CO)_{12}$[11] and $Co_2(CO)_8$[12] and for the organometallic derivatives $Co_3(CO)_9(CR)$[13] and $Co_2(CO)_6(RC_2R)$.[14] A multielectron oxidation peak is ob-

(1) Sappa, E.; Tiripicchio, A.; Carty, A. J.; Toogood, G. E. *Prog. Inorg. Chem.* **1987**, *35*, 437.
(2) Muetterties, E. L.; Rhodin, T. N.; Band, E.; Brucker, C. F.; Pretzer, W. R. *Chem. Rev.* **1979**, *79*, 91.
(3) Holt, E. M.; Whitmire, K. H.; Shriver, D. F. *J. Am. Chem. Soc.* **1982**, *104*, 5621.
(4) Carty, A. J.; MacLaughlin, S. A.; Van Wagner, J.; Taylor, N. J. *Organometallics* **1982**, *1*, 1013.
(5) (a) Dahl, L. F.; Smith, D. L. *J. Am. Chem. Soc.* **1962**, *84*, 2450. (b) Gervasio, G.; Rossetti, R.; Stanghellini, P. L. *Organometallics* **1985**, *4*, 1612.
(6) Wade, K. *Adv. Inorg. Chem. Radiochem.* **1976**, *18*, 1.
(7) Lyons, L. J.; Wang, J.; Crespi, A. M.; Sabat, M.; Harris, S.; Woodcock, C.; Shriver, D. F. *Abstracts of Papers*, 200th National Meeting of the American Chemical Society Washington, DC, Aug 1990; American Chemical Society: Washington, DC 1990; INORG 119.
(8) Jund, R.; Rimmelin, J.; Gross, M. *J. Organomet. Chem.* **1990**, *381*, 239.
(9) Pétillon, F. Y.; Rumin, R.; Talarmin, J. *J. Organomet. Chem.* **1988**, *346*, 111.
(10) Since CH_2Cl_2 is a relatively low polar solvent, problems have arisen from the *iR* drop even if a positive-feedback device has been routinely employed. All the ΔE_p values have been corrected assuming the ferrocene internal standard should have ΔE_p = 70 mV in the overall scan rate range employed (50-2000 mV/s).
(11) Holland, G. F.; Ellis, D. E.; Trogler, W. C. *J. Am. Chem. Soc.* **1986**, *108*, 1884.
(12) Mugnier, Y.; Reco, P.; Moise, C.; Laviron, E. *J. Organomet. Chem.* **1983**, *254*, 111.
(13) (a) Kotz, J. C.; Petersen, J. V.; Reed, R. C. *J. Organomet. Chem.* **1976**, *120*, 433. (b) Bond, A. M.; Peake, B. M.; Robinson, B. H.; Simpson, J.; Watson, D. J. *Inorg. Chem.* **1977**, *16*, 410.

0276-7333/91/2310-3253$02.50/0

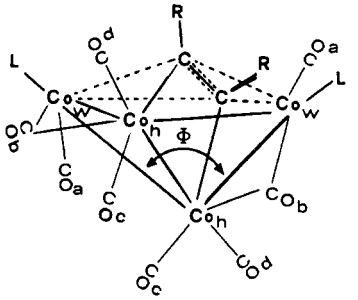

Figure 1. Butterfly clusters under study along with the labeling scheme: R = H, L = CO, **1**; R = Et, L = CO, **2**; R = Ph, L = CO, **3**; R = H, L = PPh_3, **4**. Key: w = wing-tip atoms; h = hinge atoms; Φ = dihedral angle between the wings.

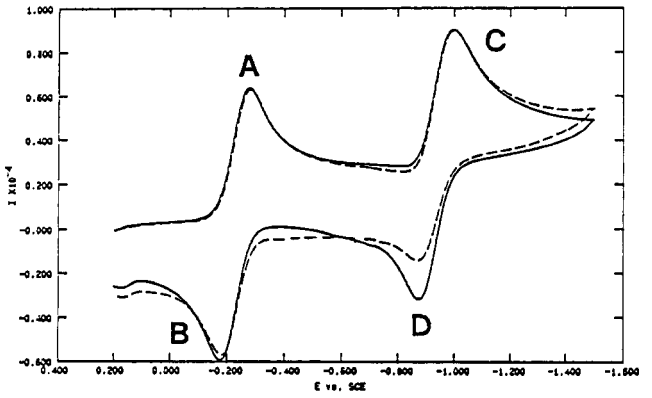

Figure 2. Cyclic voltammogram recorded at a Hg electrode on a CH_2Cl_2 solution of **1** at room temperature and at 200 mV s^{-1}: dotted line, under Ar; bold line, under CO.

served at ca +1.3 V, followed by electrochemical responses typical of insoluble materials adsorbed onto the electrode and finally by anodic stripping of metallic Co from the Pt electrode. This oxidation process has been described in detail recently[14b] and is not diagnostic at all. We then went on to investigate the cathodic response at a Hg electrode.

Under Ar atmosphere, all the butterfly clusters **1–3** exhibit two consecutive reduction peaks, A and C, with associated reoxidation peaks, B and D, respectively (Figure 2, dotted line).

Analysis of the usual electrochemical parameters[15] of the first A/B and second C/D peak systems with the scan rate, i.e., the difference from the anodic and cathodic peak potentials, $\Delta E_p = E_p^a - E_p^c$, and the ratio between the anodic and cathodic peak current, i_p^a/i_p^c, indicates the following:

(1) The first reduction step is *electrochemically* (the increase in ΔE_p with scan rate parallels that of the standard ferrocene/ferrocenium couple) and *chemically* ($i_p^a/i_p^c \simeq 1$, even at the lowest scan rate) reversible.

(2) The second reduction step is followed by a chemical reaction (i_p^a/i_p^c being 0.4 at 50 mV/s and reaching the unity at 2.0 V/s). Moreover, the ΔE_p value increases with the scan rate from 100 mV at 50 mV/s to 300 mV at 2 V/s, indicating a *quasi*-reversible electron-transfer process.

Furthermore, in the reverse scan a broad, apparently reversible, peak system can be observed a ca. +0.15 V only if the applied potential has traversed that of peak C. Inspection of literature data[14a] and deliberate addition to the solution of $[(Ph_3P)_2N][Co(CO)_4]$ salt indicate that this peak system can be assigned to the oxidation of $Co(CO)_4^-$. Indeed, this monoanion is a fragment commonly encountered in the electrochemical reduction of cobalt carbonyls.[16]

Table I. Formal Electrode Potential (V vs SCE) of the Butterfly Clusters 1–4 in CH_2Cl_2 at a Hg Electrode

complex	no.	$E^{\circ\prime}(0/1-)$	$E^{\circ\prime}(1-/2-)$
$Co_4(CO)_{10}(HC_2H)$	1	−0.331	−1.030
$Co_4(CO)_{10}(PhC_2Ph)$	2	−0.204	−0.913
$Co_4(CO)_{10}(EtC_2Et)$	3	−0.362	−1.050
$Co_4(CO)_8(PPh_3)_2(HC_2H)$	4	−0.815	−1.418

The peak currents of the two consecutive reduction processes are almost equal. Controlled-potential coulometry at the first reduction step (E_w = −0.4 V) indicates that the first, fully reversible, process consumes 1 faraday/mol of **1**. Then, in CV time scale the butterfly clusters undergo two consecutive 1e reductions, the relative formal potentials, $E^{\circ\prime} \approx (E_p^a + E_p^c)/2$, being collected in Table I. On the other hand, controlled-potential coulometry at E_w = −1.1 V, at room temperature and under Ar atmosphere, indicates that the overall reduction consumes ca. 3.5 faradays/mol of **1**. This implies that in the longer electrolysis time scale the primarily electrogenerated dianion $[Co_4(CO)_{10}(HC_2H)]^{2-}$ fragments, in addition to $Co(CO)_4^-$, to other species that are further electroreducible at the working potential.

Since room-temperature exhaustive electrolysis of **1** at E_w = −1.1 V causes complete breakdown of the cluster, we decreased the temperature from +25 to −20 °C. As expected, this enhances the lifetime of the electrogenerated dianion (1^{2-}). The CV response shows that at −20 °C the i_p^a/i_p^c ratio reaches unity at a scan rate as slow as 300 mV/s.

A further stabilization of the dianion (1^{2-}) can be achieved by using CO in lieu of Ar atmosphere (Figure 2, bold line); the i_p^a/i_p^c ratio reaches unity at room temperature under CO at a scan rate as slow as 200 mV/s. The rupture or at least the stretching of a Co–CO bond should then be involved in the rate-determining step of the decomposition of the dianion (1^{2-}). A similar path has been proposed[7] for the reduction of the isoelectronic cluster $Ru_4(CO)_{12}(PhC_2Ph)$, and the product of the two electron reductions and the following chemical step has been identified as $[Ru_4(CO)_{11}(PhC_2Ph)]^{2-}$.

The stabilization of butterfly dianions under an atmosphere of CO can be further examined by analyzing the square-wave voltammetric[17] (SWV) response of $Co_4(CO)_{10}(PhC_2Ph)$ (**3**). Our approach to the SWV technique is purely qualitative and consists of comparing the net current peaks of the first and second redox processes under Ar (Figure 3a) and under CO (Figure 3b), respectively. In Figure 3a the SWV responses in direct scan (from 0 to −1.4 V) and in reverse scan (from −1.4 to 0 V) are reported. The 1−/2− net current peaks are lower than the corresponding 0/1− ones due to the decomposition of the dianion (3^{2-}). On the contrary, since CO atmosphere stabilizes the dianion (3^{2-}) and then renders the 1−/2− process electrochemically and chemically reversible, the redox peaks of the two processes are fairly similar (Figure 3b).

The electrochemistry of clusters **1–3** (Table I) is similar to that reported for the isoelectronic $[MCo_3(CO)_{10}$-

(14) (a) Arewgoda, M.; Rieger, P. H.; Robinson, B. H.; Simpson, J.; Visco, S. J. *J. Am. Chem. Soc.* **1982**, *104*, 5633. (b) For a recent discussion of the oxidation behavior of $Co_2(CO)_6(RC_2R)$ complexes and the electrode fouling problems, see: Osella, D.; Stein, E.; Jaouen, G.; Zanello, P. *J. Organomet. Chem.* **1991**, *401*, 37.

(15) (a) Bard, A. J.; Faulkner, L. L. *Electrochemical Methods*; Wiley: New York, 1980. (b) Brown, E. R.; Sandifer, J. R. In *Physical Methods of Chemistry*; Rossiter, B. W., Hamilton, G. F., Eds.; Wiley: New York, 1986; Vol. II, Chapter IV.

(16) Colbran, S. P.; Robinson, B. H.; Simpson, J. *J. Organomet. Chem.* **1984**, *265*, 199 and references therein.

(17) O'Dea, J. J.; Osteryoung, J.; Osteryoung, R. A. *Anal. Chem.* **1981**, *53*, 695.

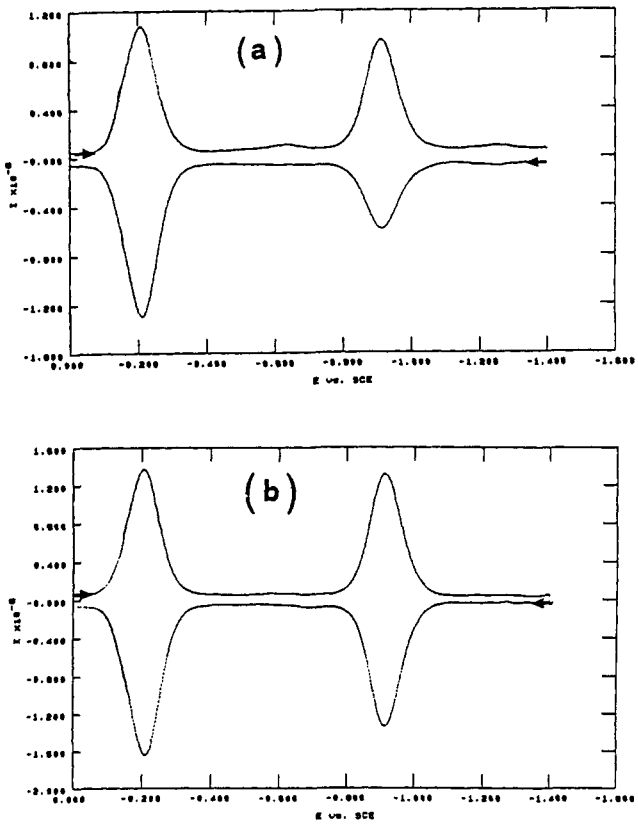

Figure 3. Square-wave voltammetric response of a CH_2Cl_2 solution of **3** at a mercury-plated gold electrode and at room temperature: (a) under Ar; (b) under CO. Conditions: frequency, 15.0 Hz; step increment, 2 mV; pulse height, 25 mV.

$(PhC_2Ph)]^-$ (M = Fe, Ru)[8] anions. The reduction potentials are shifted cathodically, as expected, by the presence of a negative charge on the butterfly cluster, and the chemical decomposition of the dianion is somewhat faster. This is in accord with the higher instability of heterometallic cluster ions when compared with that of homometallic counterparts.[18]

At low temperature and under an atmosphere of CO, it is possible to stabilize the dianion 1^{2-} and then to follow its fate. Exhaustive electrolysis at E_w = −1.2 V at −20 °C and under CO consumes exactly 2 faradays/mol of **1**, indicating that under these experimental conditions the decomposition of 1^{2-} is inhibited; in other words, the complete chemical reversibility is achieved. Then, the potential is disconnected, the CO replaced by Ar, and the temperature allowed to rise to 25 °C. The dianion $[Co_4(CO)_{10}(HC_2H)]^{2-}$ decomposes to $Co(CO)_4^-$ (identified by the strong IR adsorption at 1890 cm^{-1}) and to $Co_2(CO)_6(HC_2H)$ identified by IR spectroscopy and TLC comparison with an authentic sample).[19]

The fact that $Co_2(CO)_6(HC_2H)$ is electroreducible (in a chemically irreversible way) at a potential (E_p = −1.05 V)[14b] less cathodic than the working one (E_w = −1.2 V) partially accounts for the excess of charge consumed and for the complete decomposition of $Co_4(CO)_{10}(HC_2H)$ in the room-temperature electrolysis.

Figure 4 shows the 100 K ESR spectrum of a CH_2Cl_2 solution of **1** exhaustively electrolyzed at E_w = −0.7 V (mercury pool) at −20 °C and under CO.

A broad absorption is observed at g = 2.057 (±0.003), having a peak to peak separation, ΔH_{pp}, of 252 (±2) G. No hyperfine or superhyperfine coupling can be detected. These features suggest that the odd electron is delocalized over the Co_4 core in the radical anion 1^-. This proposal is consistent with the character of the LUMO found in the theoretical calculations (vide infra).

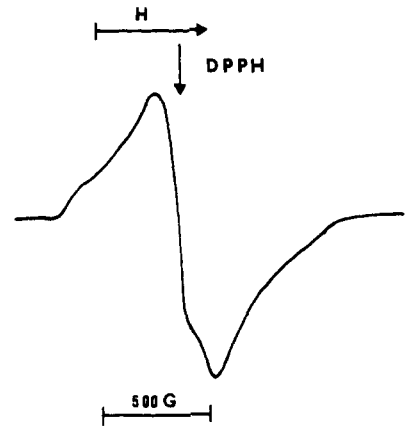

Figure 4. X-band 100 K ESR spectrum of a dichloromethane solution of 1^- electrogenerated at a mercury pool (E_w = −0.4 V) at −20 °C under CO.

Scheme I

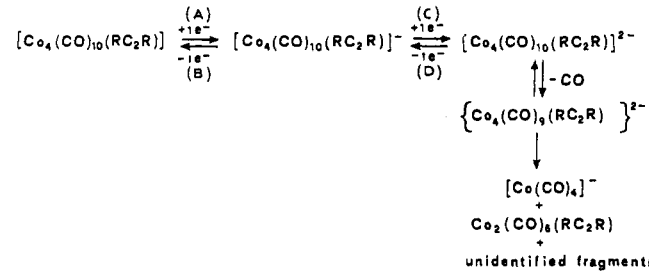

When the working potential of the electrolysis (at −20 °C and under CO) is set at −1.1 V, the ESR signal of the radical monoanion decreases, but does not completely disappear even when 2 faradays/mol is consumed. This indicates partial disproportionation of the dianion (1^{2-}) to monoanion (1^-). Several other small signals are evident in the ESR spectrum, indicating extensive fragmentation.[20]

The overall electrochemical mechanism is depicted in Scheme I. Unfortunately, the full stoichiometry remains unknown, since not all the fragmentation products could be identified.

In order to clarify the mechanism of decomposition of dianion, we have synthesized the disubstituted cluster $Co_4(CO)_8(PPh_3)_2(HC_2H)$ (**4**) by using a previous literature procedure[21] in which the molecular formula of **4** was reported on the basis of elemental analysis and molecular weight determination.

The ^1H NMR spectrum of **4** shows a triplet at 7.82 ppm assigned to two equivalent CH groups coupled to two equivalent P nuclei. In addition, there are two multiplets centered at ca. 7.6 and 7.1 ppm, assigned to the phenyl groups. The triplet and the two multiplets exhibit an integrated intensity ratio of 2/30, consistent with the molecular formula suggested.[21]

The ^{31}P NMR spectrum confirms that the two PPh_3 ligands are equivalent; there is a broad resonance at ca. 46 ppm. The broadening is consistent with the rapid relaxation[22] induced by the quadrupolar Co nuclei (I = $^7/_2$).

(18) Lindsay, P. N.; Peake, B. M.; Robinson, B. H.; Simpson, J.; Honrath, U.; Vahrenkamp, H.; Bond, A. M. *Organometallics* **1984**, *3*, 413.
(19) Dickson, R. S.; Fraser, P. J. *Adv. Organomet. Chem.* **1974**, *12*, 323.
(20) Casagrande, L. V.; Chen, T.; Rieger, P. H.; Robinson, B. H.; Simpson, J.; Visco, S. J. *Inorg. Chem.* **1984**, *23*, 2019.
(21) Iwashita, Y.; Tamura, F.; Wakamatsu, H. *Bull. Chem. Soc. Jpn.* **1970**, *43*, 1520.

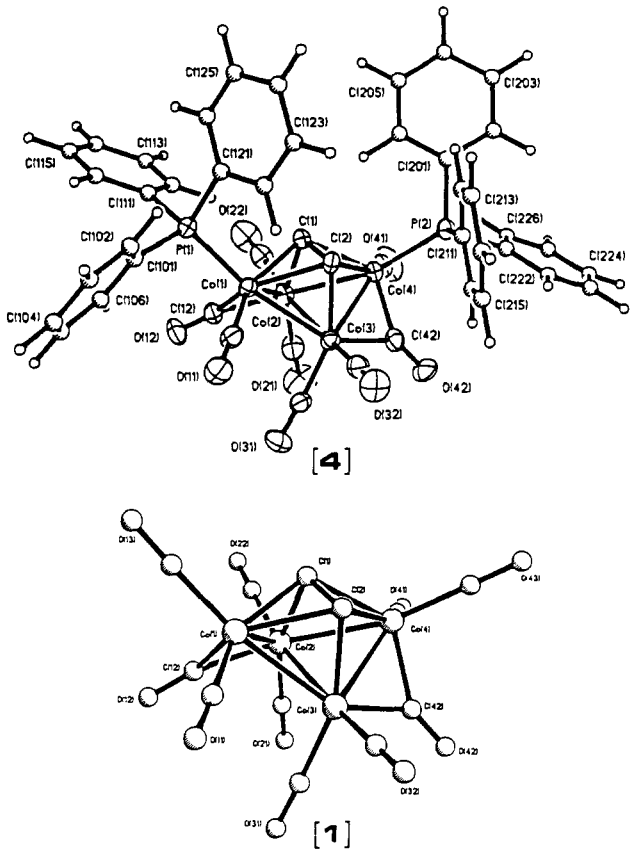

Figure 5. Crystal structures of 4 and 1. (a) Molecular plot of 4 along with the atom-numbering scheme. Thermal ellipsoids are drawn at the 50% probability level. (b) Molecular plot of 1[5] in the same orientation and with the same atom numbering scheme as for 4 for comparison.

The $^{13}C\{^1H\}$ NMR spectrum in the organic region shows a very broad resonance at ca. 145.2 ppm, attributable to two equivalent ≡CH groups along with the usual pattern of six equivalent phenyl groups. We have synthesized the ^{13}CO-enriched samples of the parent compound 1 and of the diphosphine derivative 4 (ca. 25% enrichment level). The ^{13}C NMR spectrum of 1 at −75 °C, in the CO region, shows three resonances at 205.2, 198.3, and 191.2 ppm in an integrated intensity ratio of 6/2/2. They broaden, collapse in the base line, and eventually merge in a single, broad resonance as the temperature is raised. The low-temperature spectrum has been previously interpreted[23] as a result of the opening of the Co_h–$(CO)_a$ bonds and the localized scrambling of the resulting $Co_w(CO)_3$ units (Figure 1) while the $Co_h(CO)_2$ moieties remain rigid.

The ^{13}C NMR spectrum of 4 shows a similar pattern at −30 °C, indicating that the barrier to fluxionality has risen by the presence of the bulky PPh_3 ligands. Three resonance at 192.9, 176.3, and 169.6 ppm are observed in an integrated intensity ratio of 4/2/2. Provided that the actual dynamic process[23] is unchanged on passing from 1 to 4, this ratio suggests that the PPh_3 substitution for CO has occurred on the wing-tip atoms. This is in accord with the high symmetry previously suggested by the other NMR spectra. In order to assess the precise geometry of 4, a single-crystal X-ray determination has been undertaken.

The molecular structure of 4 is illustrated in Figure 5. The overall molecular geometry is closely related to that of the unsubstituted parent complex 1,[5b] which is also depicted in Figure 5. Disubstitution of CO by PPh_3 has occurred regiospecifically on the wing-tip atoms, and the two phosphine substituents occupy trans-equatorial sites on the Co_w atoms, giving the molecule approximate C_2 symmetry. The phosphines are pseudo-trans to the unbridged Co_w–Co_h edges, with the phosphorus atoms, P(1) and P(2), lying close to the Co(1)Co(2)Co(3) (deviation 0.51 Å) and Co(2)Co(3)Co(4) (deviation 0.54 Å) planes, respectively. This is the normal site of phosphine substitution in other butterfly clusters, as evidenced by previous crystal structure determinations.[24] The phosphine, being a better and bulkier nucleophile than the carbonyl ligand, prefers a metal center with a lower formal coordination from both a steric and the electronic viewpoint. The positioning of the phosphine trans to a metal–metal edge avoids direct competition with a trans carbonyl (a strong π-acceptor ligand) for π-electron density from the same metal orbital.

A comparison of the selected distances and bond angles of 1[5b] and 4 indicates that the same trends are present in both (Table II). The Co(2)–Co(3) "hinge" edge is ca. 0.10 Å longer than the Co_h–Co_w edges in both structures, and there is good agreement between the individual Co–Co edge lengths in both structures. The presence of bridging carbonyls spanning the Co(1)–Co(2) and Co(3)–Co(4) edges does not exert a shortening influence, as observed in some other cluster systems, since these distances are not significantly different from the two unbridged edges. The bridging carbonyl ligands show a slightly greater asymmetry in 4 than in 1, with the shorter Co–C bonds associated with the phosphine-substituted wing-tip metals. The bond parameters for the remaining eight terminal carbonyls and the orientation of the alkyne chain are similar in the two structures. In both complexes 1 and 4 the alkyne C–C vector is slightly skewed with respect to

Table II. Comparison between the Selected Bond Distances (Å) and Bond Angles (deg) of $Co_4(CO)_{10}(HC_2H)$ (1)[5] and $Co_4(CO)_8(PPh_3)_2(HC_2H)$ (4)

	1	4
	Distances	
Co(1)–Co(2)	2.446 (1)	2.438 (2)
Co(1)–Co(3)	2.469 (1)	2.447 (2)
Co(1)–Co(4)	3.558 (1)	3.568 (2)
Co(2)–Co(3)	2.559 (1)	2.562 (1)
Co(2)–Co(4)	2.459 (1)	2.469 (2)
Co(3)–Co(4)	2.454 (1)	2.448 (2)
C(1)–C(2)	1.399 (7)	1.394 (11)
Co(1)–C(1)	2.038 (5)	2.045 (8)
Co(1)–C(2)	2.095 (5)	2.122 (8)
Co(2)–C(1)	1.982 (5)	1.992 (10)
Co(3)–C(2)	1.982 (5)	1.991 (9)
Co(4)–C(1)	2.094 (5)	2.128 (8)
Co(4)–C(2)	2.038 (5)	2.032 (8)
Co(1)–P(1)		2.208 (3)
Co(4)–P(2)		2.223 (3)
Co(1)–C(12)	1.882 (6)	1.837 (11)
Co(2)–C(12)	2.022 (5)	2.043 (9)
Co(3)–C(42)	1.988 (5)	2.005 (10)
Co(4)–C(42)	1.895 (6)	1.865 (10)
	Angles	
Co(2)–C(1)–C(2)	106.6 (3)	106.6 (6)
Co(3)–C(2)–C(1)	107.4 (3)	107.3 (7)
Co(1)–C(1)–Co(4)	118.9 (2)	117.6 (4)
Co(1)–C(2)–Co(4)	118.9 (2)	118.4 (4)
P(1)–Co(1)–Co(3)		162.1 (1)
P(2)–Co(4)–Co(2)		164.5 (1)
dihedral angle Φ	116	117

(22) Aime, S.; Gobetto, R.; Osella, D.; Milone, L.; Hawkes, G. E.; Randall, E. W. *J. Magn. Reson.* **1988**, *65*, 308.

(23) (a) Evans, J.; Johnson, B. F. G.; Lewis, J.; Matheson, T. W.; Norton, J. R. *J. Chem. Soc., Dalton Trans.* **1978**, 626. (b) Aime, S.; Milone, L.; Sappa, E. *Inorg. Chim. Acta* **1976**, *16*, L7.

(24) Raithby, P. R. In *Transition Metal Clusters*; Johnson, B. F. G., Ed.; Wiley, New York, 1980; Chapter 2.

Scheme II

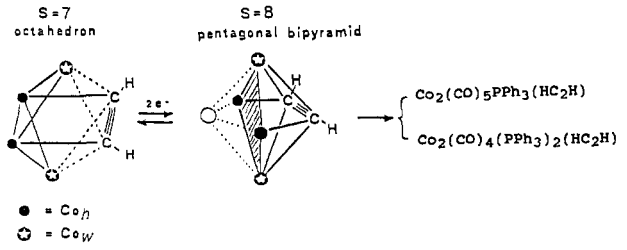

the Co_4 framework about the molecular 2-fold axis that passes through the midpoint of the C(1)–C(2) and Co(2) and Co(3) vectors, consistent with the idealized C_2 point group for the two molecules. Significantly, the dihedral angle (Φ) between the butterfly wings in 1 and 4 is very similar, which does not reflect any change in electron density on the cluster core resulting from the substitution of two carbonyls in 1 by two phosphines in 4. Finally, the two Co–P distances (average 2.216 Å) are similar to the weighted mean value of 2.211 Å reported for such a bond.[25]

The electrochemistry of 4 is qualitatively similar to that of the parent cluster 1, both formal reduction potentials $E^{\circ\prime}$ being shifted cathodically by about 500 mV. This shift is consistent with the substitution of two PPh_3 ligands (having a higher σ donor/π acceptor ratio) for CO.[11] The fact that the reduction potentials are sensitive to the electronic effect of the ligands on the Co_4 core but almost insensitive to the electronic nature of the alkyne substituents (Table I) suggests, once again, that the reduction processes concern mainly the metallic core. The difference between the formal electrode potentials in the two subsequent cathodic reductions, $\Delta E^{\circ\prime} = E^{\circ\prime}(0/1-) - E^{\circ\prime}(1-/2-)$, is of the order of 600 mV, regardless of the substituents of the alkyne or of the Co_4 core, the solvent, and the electrode material. The constant difference in all the derivatives 1–4 suggest that the both electrons are added to a nondegenerate LUMO. This difference can be assumed to represent, to a first approximation, the energy required to overcome electronic repulsion within the same MO (ca. 58 kJ/mol). A similar value has been found for homo- and heterometallic C-, Ge-, or P-capped trinuclear clusters[18] and for the $Fe_3(CO)_8(alkyne)_2$ series.[26]

As with the parent compound 1, the chemical reversibility of the second reduction step of 4 can be enhanced by lowering the temperature and using CO atmosphere. Indeed, exhaustive electrolysis of 4 at $E_w = -1.5$ V, at −20 °C and under CO, consumes 2 faradays/mol (no chemical complication). Then, the potential is disconnected and 4^{2-} allowed to decompose, as in the previous experiment on 1^{2-}. The bimetallic complexes are identified as $Co_2(CO)_5(PPh_3)(HC_2H)$ and $Co_2(CO)_4(PPh_3)_2(HC_2H)$ by IR and ^1H NMR spectroscopy and by TLC comparison with authentic samples,[27] in an approximate 2/1 molecular ratio.

Provided there is no intermolecular or intramolecular exchange of PPh_3 groups during the decomposition process of the dianion (4^{2-}), the absence of the $Co_2(CO)_6(HC_2H)$ complex in the decomposition products indicates that the Co_h–Co_h bond is preferentially broken during the second reduction step. This is consistent with the Co_h–Co_h antibonding character of the LUMO (vide infra).

Interestingly, the ESR spectrum of the radical monoanion (4^-) at 100 K is very similar to that of 1^-, exhibiting a broad absorption at $g = 2.029 \pm 0.003$, having a $\Delta H_{pp} = 265 \pm 2$ G.

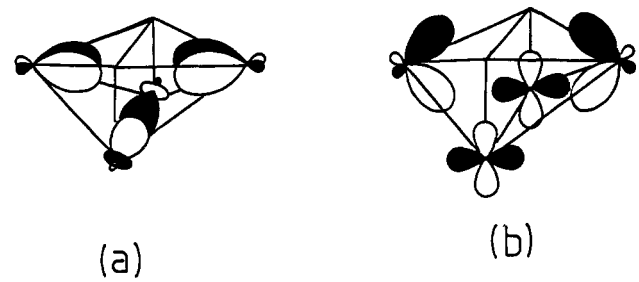

Figure 6. Schematic representation of the two lowest lying unoccupied MOs of $Co_4(CO)_{10}(HC_2H)$ (1): (a) MO 74 (LUMO); (b) MO 75.

The second reduction step should be associated to a geometrical change according to the larger ΔE_p value. Within the PSEP approach we can suggest that a cluster expansion from closo octahedral ($S = 7$, $n = 6$) to nido pentagonal bipyramid ($S = 8$, $n = 6$) geometry occurs concomitant the second reduction process (Scheme II) and this cluster expansion likely involves the breaking or at least the stretching of a Co–CO bond. Then the unstable nido cluster dianion collapses to $Co(CO)_4^-$ and to the bimetallic fragments $Co_2(CO)_5(PPh_3)(HC_2H)$ and $Co_2(CO)_4(PPh_3)_2(HC_2H)$.

The bonding in $Co_4(CO)_{10}(HC_2H)$ has previously been explored by use of the Fenske–Hall technique,[28] and thus in this work we concentrate only on the characteristics of those MO's that may provide some insight into (i) the observed electrochemistry of the tetracobalt butterfly cluster and (ii) the pattern of phosphine substitution. The results of the molecular orbital analysis of $Co_4(CO)_{10}(HC_2H)$ illustrate that the two lowest lying unoccupied MO's are predominantly metal in character (Figure 6). The LUMO, MO 74, possesses approximately equal contributions from each metal atom (ca. 18% per Co); a nodal plane runs through the Co_4 butterfly framework, thereby rendering MO 74 Co_h–Co_h antibonding. MO 75 (quite close in energy to the LUMO) is bonding along the Co_h–Co_h vector but has Co_h–Co_w antibonding character. Thus, on reduction, occupancy of either MO 74 or 75 will be expected to lead to a weakening of the Co–Co bonding within the butterfly framework. The theoretical results are consistent with reduction leading to a perturbation of the tetracobalt core rather than of any other (e.g., alkyne) part of the molecule.

Finally, the calculated Mulliken atomic charges for $Co_4(CO)_{10}(HC_2H)$ show the wing-tip cobalt atoms to be more positively charged ($q = +0.109$) then the hinge atoms ($q = -0.014$). Thus, on charge grounds, we would expect the initial site of phosphine attack to be at a wing-tip metal atom. Substitution of phosphine for carbonyl at the equatorial site of a wing-tip cobalt atom to give the model compound $Co_4(CO)_9(PH_3)(HC_2H)$ causes a reduction in the charge at that atom from $q = +0.109$ to $q = +0.102$. The remaining unsubstituted wing-tip atom continues to carry the highest positive charge of any of the four cobalt atoms in the butterfly framework. This is consistent with concomitant substitution at both wing-tip atoms to give $Co_4(CO)_8(PR_3)_2(HC_2H)$. It is work commenting that the electronic structure of the similar model complex $Ru_4(CO)_{12}(HC_2H)$ has been obtained by CNDO quantum mechanical calculations.[29] In this case, the hinge ruthenium

(25) Orpen, A. G.; Branner, L., Allen, F. H.; Kennard, O.; Watson, D. G.; Layla, R. *J. Chem. Soc., Dalton Trans.* **1989**, 555.
(26) Osella, D.; Arman, G.; Botta, M.; Gobetto, R.; Laschi, F.; Zanello, P. *Organometallics* **1989**, *8*, 620.
(27) Iwashita, Y.; Tamura, F.; Nakamura, A. *Inorg. Chem.* **1969**, *8*, 1179.
(28) DeKock, R. L.; Deshmukh, P.; Dutta, T. K.; Fehlner, T. P.; Housecroft, C. E.; Hwang, J.L.-S. *Organometallics* **1983**, *2*, 1108.

Table III. Crystal Data for 4

formula	$C_{46}H_{32}Co_4O_8P_2$
mol wt	1010.38
crystal system	monoclinic
space group	$P2_1/n$
a, Å	11.491 (5)[a]
b, Å	24.178 (8)
c, Å	15.998 (5)
β, Å	105.84 (3)
V, Å^3	4275.9 (9)
Z	4
D(calcd), g cm^{-3}	1.569
μ(Mo Kα), cm^{-1}	16.16
F(000)	2040
T, K	290
radiation	Mo Kα (λ = 0.71069 Å)
2θ limits, deg	$5.0 < 2\theta < 45.0$
data collection (hkl)	+12,+26,±17
no. of reflcns	6063
no. of unique reflcns	5051
no. obsd reflcns ($F_o \leq 5\sigma(F_o)$)	3827
R_F[b]	0.061
R_{wF}[c]	0.061
w	$2.0765/[\sigma^2(F_o) + 0.001F_o^2]$

[a] Unit cell parameters obtained from least-squares fit of the angular settings of 48 reflections ($20 \leq 2\theta \leq 25°$). [b] $R_F = \sum(||F_o| - |F_c||)/\sum(F_o)$. [c] $R_{wF} = [\sum w(|F_o| - |F_c|)^2/\sum w(F_o)^2]^{1/2}$.

atoms have higher positive charge in respect to their wing counterparts. The photochemical substitution of more basic phosphine or phosphite for CO occurs regiospecifically on a wing-tip atom,[30] likely because of steric constraints, but only monosubstituted compounds, namely $Ru_4(CO)_{11}(PR_3)$(alkyne), can be obtained.

Experimental Section

The compounds $Co_4(CO)_{10}$(alkyne) (1–3) were synthesized according to literature procedures[19] and their identities confirmed by IR and ^{1}H NMR spectroscopy on a Perkin-Elmer 580B and a Jeol GX-270-89 spectrometer, respectively.

Compound 4 has been obtained[21] in almost quantitative yield by stirring a mixture of 1 and PPh_3 in 1/2 molecular ratio in dichloromethane at room temperature under N_2 for 15 min. Compound 4 was then crystallized from hexane/dichloromethane (9/1).

The ESR spectra were obtained from a Bruker 200 D-SCR instrument operating at 9.78 GHz (X-band) equipped with a variable-temperature ER 411 VT unit.

Voltammetric measurements were performed with two sets of instrumentation: a PAR 273 electrochemical analyzer connected to an interfaced IBM microcomputer and a BAS 100 electrochemical analyzer.

A three-electrode cell was designed to allow the tip of the reference electrode (SCE) to closely approach the working electrode. Compensation for the iR drop was applied through positive-feedback device. All measurements were carried out under nitrogen in anhydrous deoxygenated solvents. Solution concentrations were 1×10^{-3} M for the compounds under study and 1×10^{-1} M for the supporting electrolyte, $[Et_4N]ClO_4$. The temperature of the solution was kept constant (±1 °C), by circulation of a thermostated water/ethanol mixture through a jacketed cell. The working electrode was a gold disk amalgamated by dipping in mercury (area ca. 0.8 mm^2).

Potential data (vs SCE) were checked against the ferrocene (0/1+) couple; under the actual experimental conditions the ferrocene/ferrocenium couple is located at +0.49 V in dichloromethane.

The number of electrons transferred (n) was determined by controlled-potential microcoulometry at a mercury pool. The working potential (E_w) for reduction process was ca. 0.1 V negative of the corresponding electrode potential (E_p); all coulometric experiments were done in duplicate.

Table IV. Atomic Coordinates (×10^4) and Equivalent Isotropic Displacement Parameters (Å^2 × 10^3)

	x	y	z	U(eq)
Co(1)	1834 (1)	3331 (1)	3328 (1)	39 (1)
Co(2)	3671 (1)	2773 (1)	3681 (1)	42 (1)
Co(3)	1729 (1)	2439 (1)	2587 (1)	40 (1)
Co(4)	2605 (1)	1930 (1)	3935 (1)	38 (1)
P(1)	1401 (2)	4038 (1)	4064 (1)	39 (1)
C(102)	−616 (5)	4699 (2)	3214 (4)	56 (2)
C(103)	−1199	5074	2573	74 (3)
C(104)	−557	5334	2059	69 (3)
C(105)	669	5220	2187	68 (3)
C(106)	1252	4845	2828	63 (3)
C(101)	610	4585	3341	41 (2)
C(112)	3636 (6)	4101 (2)	5280 (4)	57 (3)
C(113)	4582	4362	5887	66 (3)
C(114)	4509	4925	6057	72 (3)
C(115)	3490	5227	5620	79 (3)
C(116)	2544	4966	5013	61 (3)
C(111)	2617	4403	4843	48 (2)
C(122)	−570 (5)	3466 (2)	4297 (3)	49 (2)
C(123)	−1391	3294	4745	62 (3)
C(124)	−1277	3784	5587	67 (3)
C(125)	−342	3845	5981	64 (3)
C(126)	480	4017	5533	50 (2)
C(121)	366	3827	4691	39 (2)
P92)	1568 (2)	1306 (1)	4459 (1)	40 (1)
C(202)	1397 (6)	906 (2)	6074 (4)	62 (3)
C(203)	1450	960	6952	77 (3)
C(204)	1833	1456	7384	77 (3)
C(205)	2163	1899	6938	88 (4)
C(206)	2110	1845	6060	68 (3)
C(201)	1727	1349	5628	42 (2)
C(212)	−856 (6)	1518 (3)	4452 (3)	66 (3)
C(213)	−2081	1595	4040	85 (4)
C(214)	−2518	1515	3145	80 (3)
C(215)	−1728	1359	2662	70 (3)
C(216)	−503	1281	3074	60 (3)
C(211)	−66	1361	3969	44 (2)
C(222)	1163 (5)	212 (3)	3800 (4)	69 (3)
C(223)	1507	−337	3740	84 (3)
C(224)	2639	−519	4231	71 (3)
C(225)	3426	−153	4783	72 (3)
C(226)	3082	396	4843	60 (3)
C(221)	1951	578	4352	48 (2)
C(1)	2385 (8)	2761 (3)	4300 (5)	42 (3)
C(2)	1353 (8)	2544 (3)	3720 (5)	39 (3)
C(11)	839 (9)	3530 (4)	2337 (6)	52 (4)
O(11)	199 (7)	3679 (3)	1697 (5)	74 (3)
C(12)	3300 (9)	3554 (4)	3191 (6)	49 (4)
O(12)	3879 (7)	3888 (3)	2978 (5)	67 (3)
C(21)	4536 (10)	2544 (4)	2992 (8)	66 (5)
O(21)	5108 (8)	2368 (4)	2572 (7)	113 (5)
C(22)	4934 (9)	2948 (4)	4562 (7)	61 (4)
O(22)	774 (7)	1931 (4)	88 (6)	105 (4)
C(31)	2277 (10)	2633 (4)	1690 (6)	57 (4)
O(31)	2620 (8)	2797 (3)	1126 (5)	91 (4)
C(32)	219 (10)	2298 (4)	1921 (6)	55 (4)
O(32)	−723 (7)	2222 (3)	1482 (5)	81 (3)
C(41)	4074 (10)	1663 (4)	4394 (6)	57 (4)
O(41)	5008 (7)	1482 (3)	4654 (6)	98 (4)
C(42)	2367 (9)	1665 (4)	2806 (6)	52 (4)
O(42)	2454 (7)	1290 (3)	2379 (4)	75 (3)

[a] Equivalent isotropic U defined as one-third of the trace of the orthogonalized U_{ij} tensor.

Crystal Structure Determination. Crystallographic data are collected in Table III. Suitable dark green crystals were obtained by recrystallization from toluene-saturated solution. With a crystal with dimensions 0.076 mm × 0.323 mm × 0.560 mm, accurate cell dimensions, at room temperature, were obtained by least-squares refinement of 48 accurately centered reflexions ($20 < 2\theta < 25°$) on a Stoe-Siemens four-circle diffractometer equipped with graphite-monochromated Mo radiation. Data collection was performed by employing a 30-step w/θ scan mode with a step width of 0.03° and step time in the range 1.0–4.0 s/step.

(29) Granozzi, G.; Bertoncello, R.; Acampora, M.; Ajò, D.; Osella, D.; Aime, S. *J. Organomet. Chem.* **1983**, *244*, 383.
(30) Osella, D.; Aime, S.; Nicola, G.; Amadelli, R.; Carassiti, V.; Milone, L. *J. Chem. Soc., Dalton Trans.* **1984**, 349.

No significant variations were observed in the three check reflections during data collection. A numerical absorption correction was applied to the data on the crystal faces (010, 0$\bar{1}$0), (110, $\bar{1}$10), (1$\bar{1}$0, $\bar{1}$10), (10$\bar{1}$, $\bar{1}$01), and (001, 00$\bar{1}$) (transmission factors 0.886 (max) and 0.734 (min)). The intensity data were converted to F_o after correction for Lorentz and polarization effects.

Structure Solution and Refinement. The systematic absences uniquely define the space group as $P2_1/n$. The positions of the Co atoms were determined by centrosymmetric direct methods (EEES: SHELX 76).[31] The remaining non-hydrogen atoms were located from subsequent electron density difference syntheses. The structure was refined by blocked full-matrix least squares with Co, P, O, and acetylenic and carbonyl C atoms anisotropic. The phenyl rings were treated as rigid groups (d(C-C) = 1.395 Å; $\angle$(C-C-C) = 120°), and the phenyl H atoms were placed in idealized positions (d(C-H) = 1.08 Å) and allowed to ride on the relevant carbons; the H atoms were assigned a common isotropic temperature factor. The weighting scheme (Table III) was introduced and gave reasonable agreement analyses. The maximum shift/error in the final cycle of refinement was 0.02, and a difference electron density synthesis showed features only in the range +0.93 to -0.58 Å^{-3}. The final R value is 0.061 for 3827 observed data ($F_o > 5\sigma(F_o)$) for 291 parameters. Atomic scattering factors for neutral atoms and anomalous dispersion corrections were taken from ref 32 and SHELX 76[31] (P, O, C, H). All calculations were performed with use of programs in ref 31. Final atomic coordinates and equivalent isotropic displacement parameters are listed in Table IV.

Theoretical Calculations. Fenske-Hall molecular orbital calculations[33] were carried out on $Co_4(CO)_{10}(HC_2H)$ (1) with use of crystallographically determined coordinates.[5b] The calculations employed a single-ζ Slater function for the 1s and 2s functions of C and O. The exponents were obtained by curve fitting the double-ζ function of Clementi;[34] double-ζ functions for the 2p orbitals were used directly. An exponent of 1.16 was used for H. The Co 1s and 3d functions[35] were chosen for the 1+ oxidation state and were assigned by 4s and 4p functions with exponents of 2.00.

Acknowledgment. We thank the Council of National Research (CNR, Rome) and the MURST (Rome) for financial support. C.N. thanks the European Economic Community (EEC) for a studentship grant within the ERASMUS scheme.

Supplementary Material Available: Anisotropic displacement parameters (Table S1), hydrogen atom coordinates and isotropic displacement parameters (Table S2), and tables of bond distances and angles for 4 (4 pages); a table of observed and calculated structure factors for 4 (22 pages). Ordering information is given on any current masthead page.

(31) Sheldrix, G. M. *SHELX 76, Program for Crystal Structure Determination*; University of Cambridge: Cambridge, 1976.
(32) *International Tables for X-ray Crystallography*; Kynoch Press: Birmingham, England, 1974; Vol. 4, pp 91-161, 149-150.
(33) Fenske, R. F.; Hall, M. B. *Inorg. Chem.* **1972**, *11*, 768.
(34) Clementi, E. *J. Chem. Phys.* **1964**, *40*, 1944.
(35) Richardson, J. W.; Nieuwpoort, W. C.; Powell, R. R.; Edgell, W. F. *J. Chem. Phys.* **1962**, *36*, 1057.

Thermodynamic and Kinetic Stability of Bis(η^3-allyl)bis(μ_2-η^3-allyl)- and Bis(η^3-methallyl)bis(μ_2-η^3-methallyl)dimolybdenum(II) Isomers and Evidence for Their Lewis Base Catalyzed Isomerization

Reed J. Blau,* Mary S. Goetz, Ronda R. Howe, Cheri J. Smith, and Rong-Jer Tsay

Department of Chemistry, University of Texas at Arlington, Arlington, Texas 76019

Upali Siriwardane

Department of Chemistry, Southern Methodist University, Dallas, Texas 75275

Received December 3, 1990

The reactivity of $Mo_2(\mu_2$-η^3-allyl$)_2(\eta^3$-allyl$)_2$ (1) is dependent on the conformation of the bridging allyls. The green Mo_2(*endo*-μ_2-η^3-allyl)(*exo*-μ_2-η^3-allyl)(*endo*-η^3-allyl)$_2$ (1(b=en,ex)(t=en$_2$)) reacts much more rapidly than the violet Mo_2(*endo*-μ_2-η^3-allyl$)_2$(endo-η^3-allyl$)_2$ (1(b=en$_2$)(t=en$_2$)) with a variety of reagents including methanol, acetylacetone, and carbon monoxide. In fact, the violet isomer can be isolated from an isomeric mixture of $Mo_2(\mu_2$-η^3-allyl$)_2(\eta^3$-allyl$)_2$ via titration with methanol. 1(b=en$_2$)(t=en$_2$) crystallizes in the orthorhombic space group *Pbcn* with cell constants a = 8.275 (11) Å, b = 11.832 (7) Å, c = 12.862 (9) Å, V = 1259 (2) Å^3, Z = 8, and $R(F)$ = 3.01%. A comparison of crystal structures for 1(b=en,ex)(t=en$_2$) and 1(b=en$_2$)(t=en$_2$) shows significantly shorter Mo-C bonds involving the terminal allyls of the latter isomer. 1(b=en$_2$)(t=en$_2$) is isomerized to an equilibrated mixture of isomers upon the addition of a Lewis base catalyst. A comparison of COSY data for various isomers of 1 and $Mo_2(\mu_2$-η^3-methallyl$)_2(\eta^3$-methallyl$)_2$ (2) suggests that 2 exists primarily as the 2(b=en,ex)(t=en,ex) isomer (88%) with minor amounts of 1(b=en,ex)(t=ex$_2$) also present (12%).

Since the report of its discovery in 1966,[1] tetraallyldimolybdenum, $Mo_2(\mu_2$-η^3-allyl$)_2(\eta^3$-allyl$)_2$ (1), has been utilized as a precursor in the formation of catalysts for olefin[2] and alkyne metathesis,[3] propene and ethanol oxidation,[4] and the polymerization of a variety of olefins including butadiene[5] and methyl methacrylate.[6] Most recently, catalysts have been prepared by the chemisorption

(1) Wilke, G.; Bogdanovic, B.; Hardt, P.; Heimbach, P.; Keim, W.; Kröner, M.; Oberkirch, W.; Tanaka, K.; Steinrücke, E.; Walter, W.; Zimmerman, H. *Angew. Chem., Int. Ed. Engl.* **1966**, *5*, 151.
(2) Ermakov, Y. I.; Kuznetzov, B. N.; Grabovskii, Y. P.; Startzev, A. N.; Lazutkin, A. M.; Zakharov, V. A.; Lazutkina, A. I. *J. Mol. Catal.* **1976**, *1*, 93.
(3) Mortreux, A.; Petit, F.; Blanchard, M. *J. Mol. Catal.* **1980**, *8*, 97.
(4) Iwasawa, Y. In *Tailored Metal Catalysts*; Iwasawa, Y., Ed.; Reidel Publishing Co., Member Kluwer Academic Publishers Group: Boston, MA, 1986; Chapter 1.
(5) Skoblikova, V. I.; Passova, S. S.; Babitskii, B. D.; Kormer, V. A. *Vysokomol. Soedin., Ser. B* **1968**, *10*, 590.
(6) Ballard, D. G. H.; Janes, W. H.; Medinger, T. *J. Chem. Soc. B* **1968**, 1168.

0276-7333/91/2310-3259$02.50/0